DIMITRI V4 Algorithm Theoretical Basis Document: Sensor-to-simulation intercomparison over Snow Pseudo-Invariant Calibration Sites (PICS)

Reference: ARG_DIM_QA4EO_TN_Snow_PICS

Version: 1.2

Date: 12th December 2023

	Name	Company/Organization	Signature	Date
Prepared by	Bahjat Alhammoud Beatrice Berthelot Cameron Mackenzie Marc Bouvet	ARGANS Ltd (UK) Magellium (FR) ARGANS Ltd (UK) ESA/ESTEC (NL)		25/11/2023
Reviewed by	Marc Bouvet	ESA/ESTEC		
Approved by	Marc Bouvet	ESA/ESTEC		

Table of Contents

List of Figures

List of Tables

Version History

Version	Date	Main changes
1.0	10/08/2023	Document creation following the TN: RFQ-QA4EO-DIMITRI-TN-015-MAG
1.1	25/11/2023	Updated version, including: - the datasets description - BRDF-hyperspectral generation - Implementation in DIMITRI V4 - Add results
1.2	1/12/2023	Updated version, over all revision, addition of the mean ratios to table 2

Reference documents

ID	Reference
RD.1	Bouvet M., Radiometric comparison of multispectral imagers over a pseudo-invariant calibration site using a reference radiometric model, Remote Sensing of Environment 140 (2014) 141–154
RD.2	Bouvet M., DIMITRI ATBD: Sensor-to-simulation intercomparison over Pseudo-Invariant Calibration Sites , issue 1.0 (14/01/2016)
RD.3	Berthelot B., BRDF Snow surfaces model ATBD, issue 1.4, Ref: RFQ-QA4EO-DIMITRI-TN-015-MAG (16/05/2023)
RD.4	Berthelot B., Snow spectra database SAGE description, issue 1.4, Ref: RFQ-QA4EO-DIMITRI-TN-015-MAG (16/05/2023)
RD.5	Alhammoud B. and Bouvet M., DIMITRI V4 ATBD: Sensor-to-simulation intercomparison over Pseudo-Invariant Calibration Sites , issue 1.1 (30/10/2030)

Acronyms

ATBD Algorithm Theoretical Basis Document
BRDF bidirectional reflectance distribution function
Cal/Val CALibration and VALidation
CEOS Committee on Earth Observation Satellites
CNES Centre National d'Etudes Spatiales
DIMITRI The Database for Imaging Multi-spectral Instruments and Tools for Radiometric Intercomparison
DN Digital Number
ECMWF European Center for Medium-Range Weather Forecasts
ENVISAT ENVIronment SATellite
EO Earth Observation
ESA European Space Agency.
GSICS Global Space-based Inter-calibration System
IVOS Infrared and Visible Optical Sensors
MERIS Medium Resolution Imaging Spectrometer
NIR Near InfraRed
OLCI Ocean and Land Color Instrument
PARASOL Polarization & Anisotropy of Reflectances for Atmospheric Sciences coupled with Observations from a Lidar
PICS Pseudo Invariant Calibration Sites
POLDER POLarization and Directionality of the Earth's Reflectances
QA4EO Quality Assurance Framework for Earth Observation
RAA Relative Azimuth Angle
ROI region of interest
RT Radiative Transfer
RTM Radiative Transfer Model
SAA Sun azimuth angle
SWIR ShortWave InfraRed
SZA Solar Zenith Angle
TCO total column ozone

TIR	Thermal InfraRed
TOA	Top-Of-Atmosphere
VAA	viewing azimuth angle.
VIS	Visible
VNIR	Visible and Near InfraRed
VZA	Viewing Zenith Angle
WGCV	Working Group on Calibration and Validation
WV	Water Vapor

Scope of the document

This document describes the Algorithm Theoretical Basis Document (ATBD) for the simulation of the TOA reflectance observation of any sensor ingested in DIMITRI over Snow/Ice Pseudo Invariant Calibration Sites (PICS) by the so-called (ARGANS) Snow methodology implemented in DIMITRI in the framework of the ESA contract N°: 400011454/15/I-SBo and its CCN1.

1. Introduction

The Desert-PICS method has been developed by Bouvet (2014), and implemented in DIMITRI V3 and V4 using MERIS 3RP as measurements to retrieve the site-BRDF model (RD.2 and RD.5). The desert Pseudo Invariant Calibration Sites (PICS) are widely used for "*multitemporal, multiband, or multiangular calibration of optical satellite sensors"* (Cosnefroy et al. 1996).

An extension of the Desert-PICS method to Snow/Ice PICS, has been developed using the recommended CEOS invariant target Dome Concordia (Dome-C) site. Dome-C has been utilized by the calibration community for several decades for monitoring onboard sensor calibration systems as well radiometric inter-comparisons. Dome-C is a high-altitude Earth target located on the East Antarctic interior plateau, which has a permanent bright, flat, and homogeneous snow-covered surface with little aerosol, cloud cover, snowfall, and water vapor burden (Doelling et al. 2021 SPIE20210019679).

Although the surface BRDF is assumed radiometrically stable in time, it is not expected to be Lambertian. At top-of-atmosphere (TOA) reflectance level, the combination of BRDF angular variability and atmospheric temporal/angular variability leads to satellite TOA reflectance varying from acquisition to acquisition. Such atmospheric temporal variability and surface/atmospheric geometrical variations can impact the TOA signal in a significant fashion. They should be corrected for by modelling the TOA signal in order to fully exploit the Snow-PICS assumed radiometric stability for the radiometric monitoring of EO multispectral sensors.

The document consists of the following sections:

- Section 2 provides an overview of the approach proposed to simulate TOA reflectance over the Dome-C
- Section 3 describes the selection of the MERIS data for the retrieval of the Dome-C surface BRDF
- Section 4 describes the inversion of both the aerosol optical properties (and load) and the surface BRDF over the Dome-C
- Section 5 describes the generation of hyperspectral BRDFs for Dome-C from the BRDFs derived in MERIS spectral bands

- Section 6 explains how the hyperspectral BRDFs obtained to simulate hyperspectral TOA reflectances at Dome-C site and ultimately TOA reflectance from any sensor
- Section 7 describes how the hyperspectral reflectance model is run to simulate MERIS observations of the Dome-C site over the period 2006-2009.
- Section 8 discusses known limitations of the TOA simulations
- Section 9 discusses uncertainties
- Section 0 is devoted to the conclusion

2. Overview of the approach to simulated Toa reflectance over the Dome-C

A model is proposed to simulate the TOA reflectance in the visible to near-infrared (NIR) spectral range over the Dome-C PICS identified by CEOS. This model is described in Bouvet (2014). It extends through the MERIS spectral range (about 400 nm to 900 nm). It is based on a fully physical radiative transfer model simulating the coupling between a realistic atmosphere and a spectral surface Bidirectional Reflectance Distribution Function (BRDF) model parameterized by 4 free parameters. The model is 'calibrated' over Dome-C site using 4 years of MERIS observations between 2006 and 2009 included. This 'calibration' process actually consists of retrieving for the site the surface BRDF model in each MERIS spectral band. This surface BRDF model retrieval is also described in Bouvet (2014 and detailed in RD.3). The retrieval of the surface BRDF was done assuming a constant set of aerosol optical properties (so-called 'Antarctic') and a constant aerosol optical thickness at 550 nm (0.05).

3. Selection of MERIS data used to retrieve the surface BRDF model parameters over Dome-C

MERIS L1 data from the 3rd reprocessing covering a 4-year period from 01/01/2006 to 31/12/2009 were extracted from the freely available Database for Imaging Multi-spectral Instruments and Tools for Radiometric Intercomparison (DIMITRI) (http://www.argans.co.uk/dimitri/). These data consist of TOA reflectances averaged over the region of interest (ROI) in Table 1. Following Bouvet (2014), the L1 data were corrected for the instrument smile effect (irradiance correction only following Bourg et al. (2008)). They were automatically cloud screened following the MERIS-GlobCarbon scheme as per Plummer (2008). Conversely to Bouvet (2014), the data were not further visually screened. About 2111 MERIS acquisitions over Dome C site are acquired over the 4-years period. After analysis of the provided file, it results that:

- About 1480 acquisitions are valid; 631 are invalid.
- 155 acquisitions partially cover the ROI and 24 acquisitions are duplicates, consequently they are removed.
- About 1325 acquisitions could be potentially used to retrieve the BRDF.

For each acquisition, the following data are automatically extracted from the DIMITRI database: the mean TOA reflectance over ROI, the standard deviation of the TOA reflectance within the ROI, the sun and viewing direction zenith and azimuth angles (SZA, VZA, SAA, VAA), the total columnar ozone (TCO) and the total column water vapour (WV)). These TCO and WV available in the DIMITRI database correspond to the meteorological data available in the MERIS L1 products. They are data from the European Center for Medium-Range Weather Forecasts (ECMWF) operational Numerical Prediction Weather (NWP) model. They were substituted by the corresponding ECMWF ERA-Interim reanalysis data (see description in Dee et al. (2011)).

Site name	North Latitute	South Latitude	East Longitude	West Longitude
Dome-C	-74.90	-75.30	123.90	-122.90

Table 1: The definition of the region of interest over the Dome-C PICS.

3.1. Temporal variabilities of the site characteristics

The temporal evolution of the TOA reflectance is the same for the 4 years. It reaches a maximum in December when the solar elevation is the highest. There are some scatterings inside or outside the parabolic shape (depending on the spectral band) which are probably due to some changes in the snow surface roughness, or clouds contamination (Figure 1).

Although the cloud detection is performed manually it is difficult to select the acquisitions for clear sky based only on selected quick-looks. Consequently acquisitions are selected if they match the following criteria:

- Clear pixels
- Number of pixels inside the ROI > 1000
- Roi_cover =1; ROI fully covered
- Sdt(RTOA(B1) < 0.005)

Based on these criteria only 683 acquisitions are retained. The variability of the valid TOA reflectance spectra is represented in Figure 2 and its temporal variabilities shown in Figure 3.

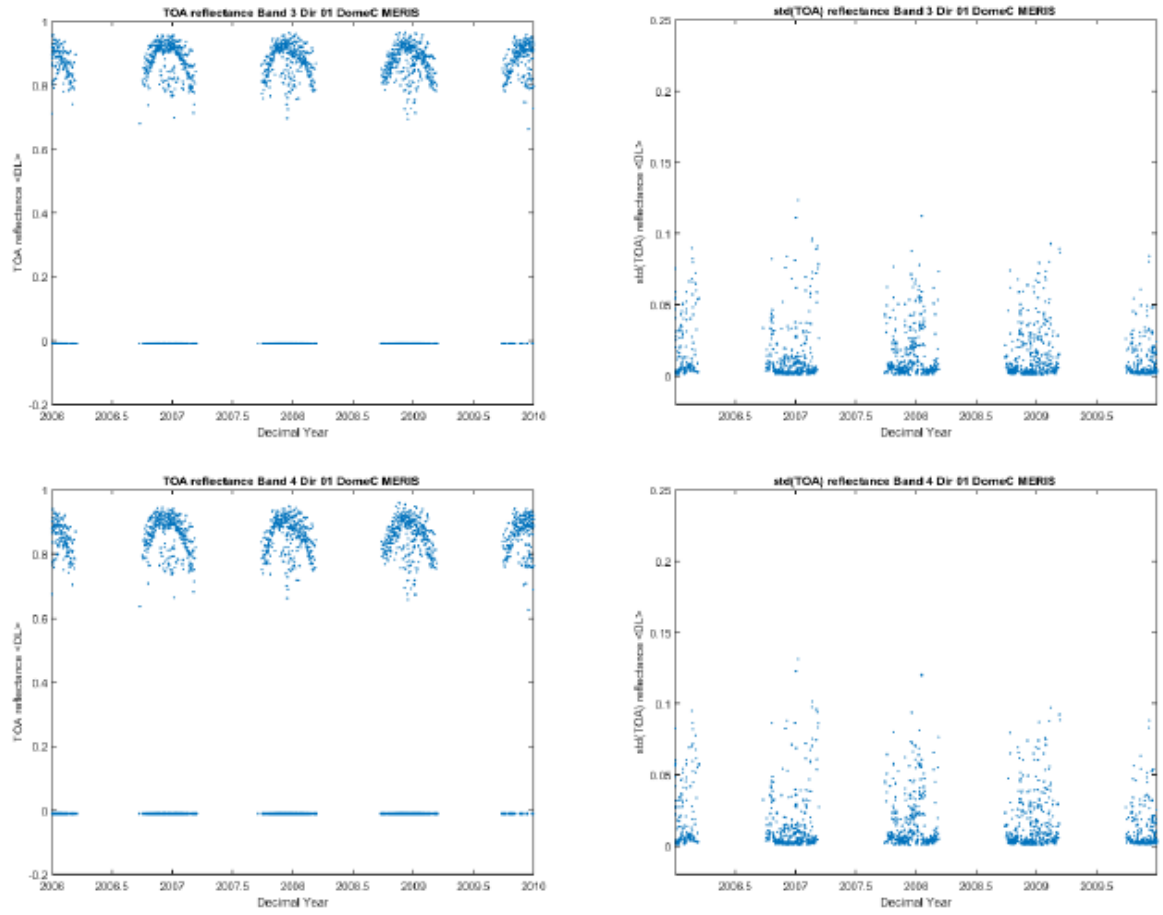

Figure 1. The temporal variability of the TOA reflectance and standard deviation for MERIS bands 3 and band 4

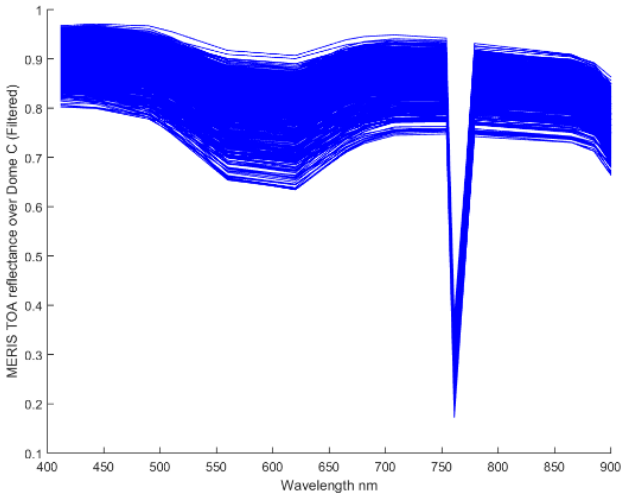

Figure 2. The TOA reflectance spectra for the time series

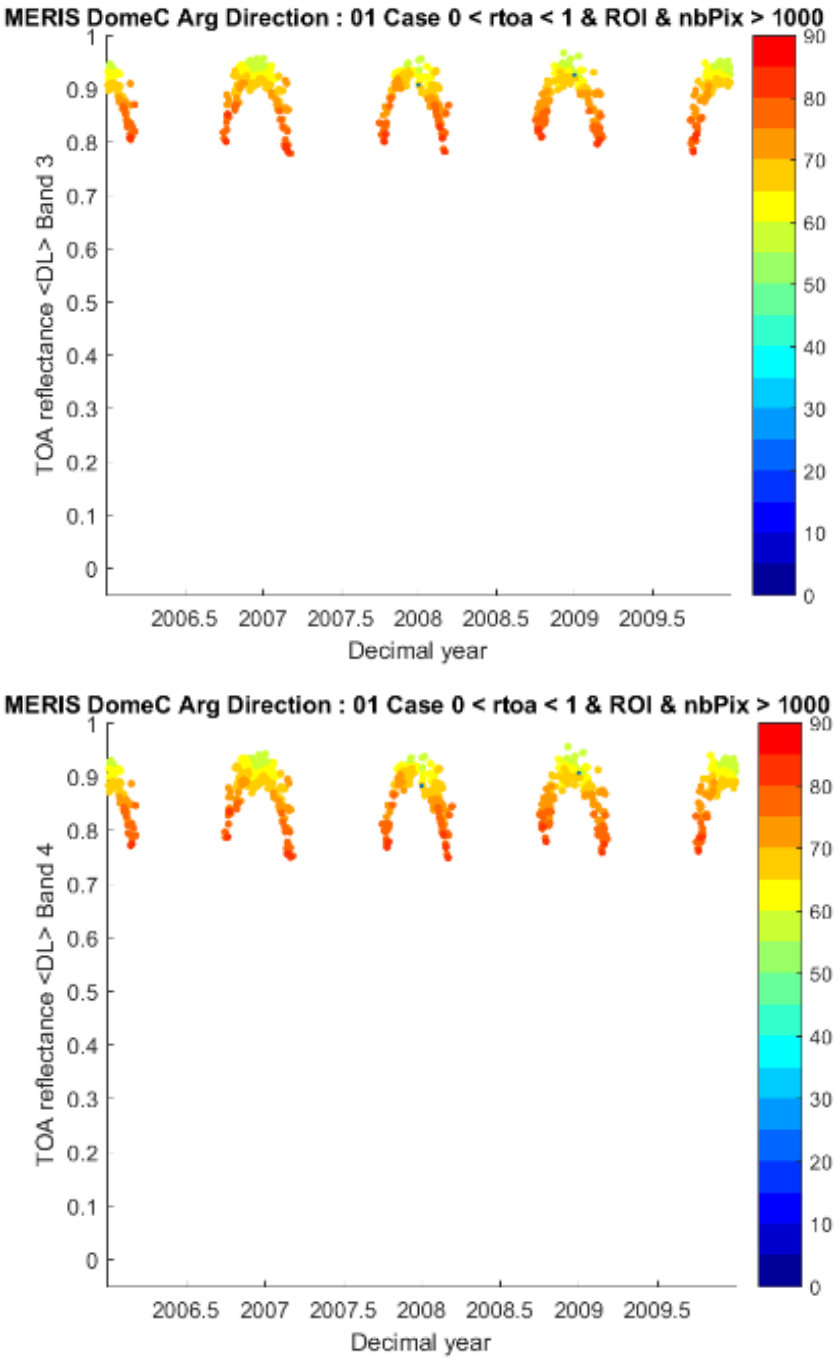

Figure 3. The temporal variability of the TOA reflectance acquired in clear sky conditions for MERIS bands 3 and band 4

4. Inversion of the surface BRDF model parameters at each MERIS spectral bands over the Dome-C PICS

In this section we describe the evolution of the surface BRDF retrieval scheme described by Bouvet (2014). For reminder, the retrieval of the surface BRDF simply is an optimisation process of the cost function described below. It consists in the retrieval of BRDF coefficients which minimised the

differences between the measured TOA reflectances and the TOA reflectances simulated by the radiative transfer model. The selected radiative transfer model used for the simulation is LibRadTran v2.0.3. The BRDF model is a modified Rahman-Pinty-Verstraete (RPV) BRDF model with 4 free parameters (Rahman et al. 1993a and b).

The inputs of LibRadtran are:

- Solver : MYSTIC (http://www.libradtran.org) (Monte Carlo) Version 1.7 for the sake of consistency with the current Desert-Methodology implemented method in DIMITRI V4.7.0
- Full treatment of polarization
- Full treatment of absorption and scattering processes
- Coupling between atmosphere and surface
- Spectral parameterization LOWTRAN
- Spectral sampling chosen: 1 nm (kurudz_1.0nm.dat)
- Antarctic Atmosphere
- OPAC Aerosol, species Antarctic, AOT 550 nm=0.05 (See Figure 4)
- RPV coefficients

Inputs card for the aerosols is

- aerosol_default
- aerosol_species_library OPAC
- aerosol_species_file Antarctic
- aerosol_set_tau_at_wvl 550.0 0.05

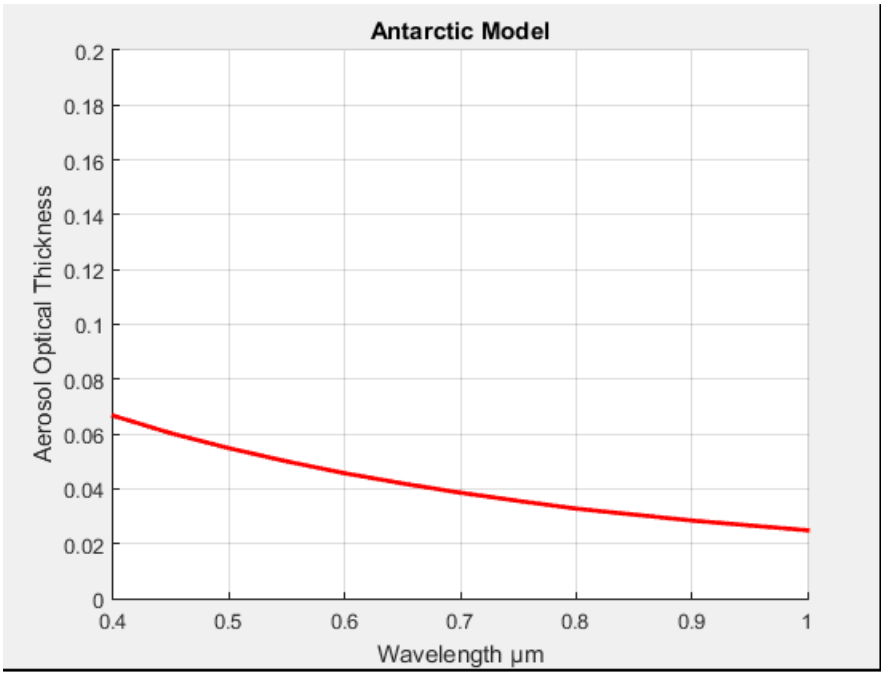

Figure 4. The Spectral variability of OPAC aerosol

4.1. Results of the inversion of the surface BRDF model parameters at the Dome-C PICS

The RPV model proposed by Rahman et al. (1993) is a parametric BRDF model representing BRDFs. It is represented by the product an amplitude ρ_0 of three separate functions accounting for both the illumination and viewing directions:

$$\rho(\theta_0,\theta_V,\Delta\phi,\rho_0,k,\Theta,\rho_c) = \rho_0\, M_1(\theta_0,\theta_V,k)\, F_{HG}(\mathrm{g},\Theta) H(\rho_c,G) \quad (1)$$

Where

$$M_1(\theta_0,\theta_V,k) = \frac{cos^{k-1}\theta_0 cos^{k-1}\theta}{(cos\theta_0+cos\theta)^{1-k}} \quad (2)$$

$$F_{HG}(\mathrm{g},\Theta) = \frac{1-\Theta^2}{(1+2\Theta cosg+\Theta^2)^{3/2}} \quad (3)$$

$$H(\rho_c,G) = 1+\frac{1-\rho_c}{1+G} \quad (4)$$

$$cosg = cos\theta_0 cos\theta + sin\theta_0 sin\theta cos\Delta\phi \quad (5)$$

$$G = (tan^2\theta_0 + tan^2\theta - 2tan\theta tan\theta_0 cos\Delta\phi)^{1/2} \quad (6)$$

where θ and θ_0 are the VZA and SZA, respectively. In the above formulation the relative azimuth angle $\Delta\phi$ is zero when the source of illumination is behind the sensor. The model is parameterized by 4 parameters: ρ_0, k, Θ and ρ_c.

The results for ρ_0, k, Θ and ρ_c at Dome-C PICS can be seen in Figure 5. On top of the at-MERIS-spectral band values of the BRDF model parameters, the retrieved hyperspectral variations are also shown in red. The derivation of the hyperspectral variations of the parameters in described in the section 5.

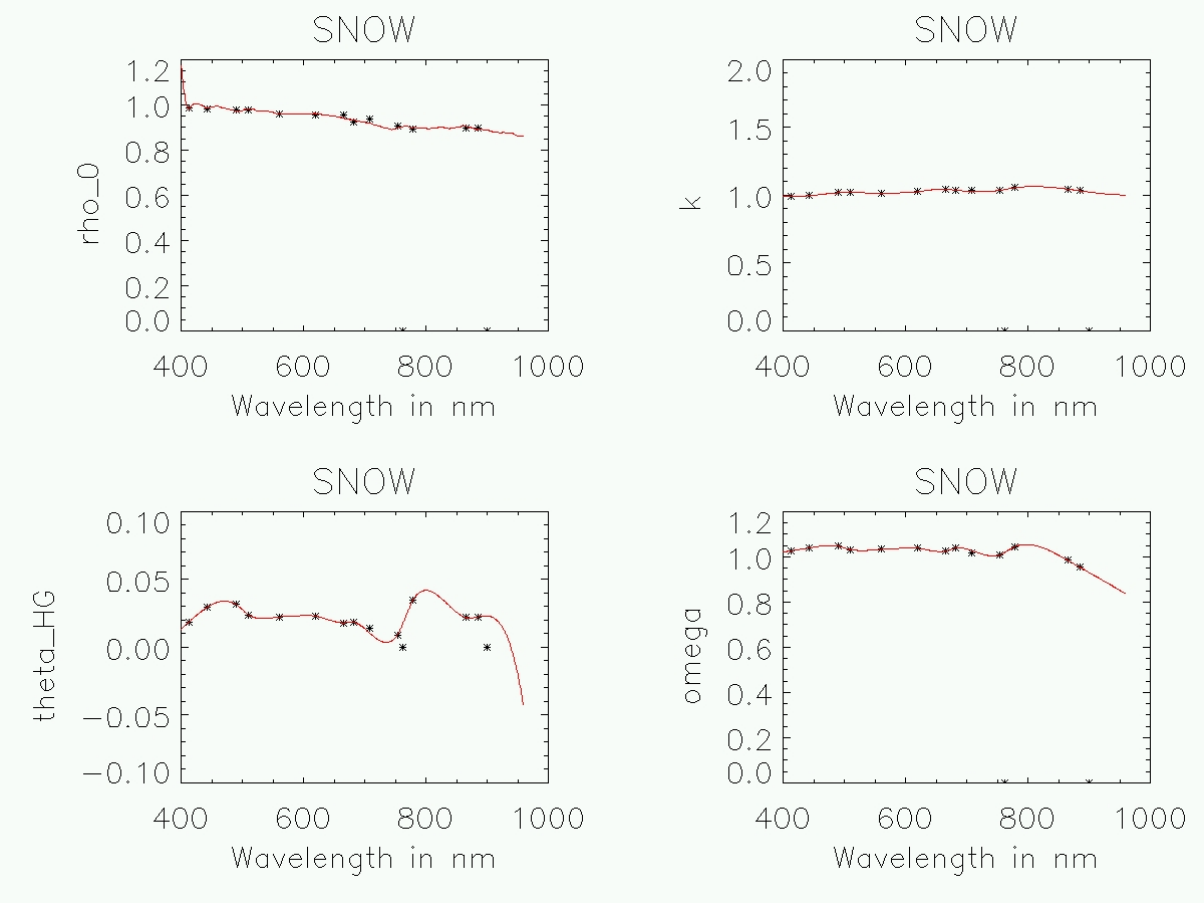

Figure 5. The spectral variations of the RPV BRDF model parameters at each MERIS spectral band inverted from the MERIS TOA reflectance observations (black stars), in red, their spectral interpolation (red line) over Dome-C PICS site, from left to right and from top to bottom, ρ_0, k, Θ and the ratio $\omega = {}^{\rho_c}/_{\rho_0}$

4.2. Analysis of the results of the inversion of the surface BRDF model parameters at the Dome-C PICS

The retrieval of the surface BRDF simply is an optimisation process of the cost function:

$$RMSE\ in\ \%(\lambda) = \chi = \sum_{i=1}^{200} \sqrt{{}^{1}/_{200} \left[\frac{\left(\rho_{sim}^{TOA}(i,\lambda) - \rho_{obs}^{TOA}(i,\lambda)\right)}{\rho_{obs}^{TOA}(i,\lambda)} \times 100 \right]^2} \qquad (7)$$

Where $\rho_{sim}^{TOA}(i,\lambda)$ and $\rho_{obs}^{TOA}(i,\lambda)$ are the simulated and observed TOA reflectance respectively and *i* is the observation index ranging from 1 to 200 and λ is the spectral band ranging from 1 to 15.

The $\rho_{sim}^{TOA}(i,\lambda)$ are derived from simulations based on the MYSTIC radiative transfer model (for details on the model, see section 3.1 of Bouvet (2014) and Berthelot (2023; RD.4)).

The statistics between the $\rho_{sim}^{TOA}(i,\lambda)$ and $\rho_{obs}^{TOA}(i,\lambda)$ obtained at the end of the surface BRDF model parameter inversion are shown in Table 2.

The accuracy (RMSE) of the modelling is good in the blues and green channels and starts to decrease in the NIR channels. The maximum relative error varies from 1% in the first channel of MERIS to 7 % in channel 14. We can also observe that the data scattering is higher in NIR channels than in the blue one.

The time-series of the relative differences between MERIS TOA reflectance for all bands and their simulations using the inverted RPV parameters are represented in Figure 6, Color code is related to the values of the SZA.

ARG MERIS								
WL (nm)	***Band***	***NB Points***	***A(0) Intercept***	***A1 Slope***	***R***	***RMSE***	***Mean Ratio***	***STD***
412	Band 1	200	-0.0767	1.0855	0.9807	0.0092	0.9995	0.0105
443	Band 2	200	-0.0104	1.0128	0.9797	0.0085	0.9988	0.0096
490	Band 3	200	0.0273	0.9685	0.9733	0.0101	1.0008	0.0118
510	Band 4	200	0.0334	0.9600	0.9785	0.0097	1.0014	0.0116
560	Band 5	200	0.0555	0.9318	0.9814	0.0111	0.9992	0.0142
620	Band 6	200	0.0384	0.9546	0.9777	0.0124	0.9970	0.0159
665	Band 7	200	0.0598	0.9300	0.9553	0.0144	0.9990	0.0176
681	Band 8	200	0.1001	0.8851	0.9517	0.0143	0.9974	0.0169
708	Band 9	200	0.0229	0.9743	0.9963	0.0035	0.9990	0.0040
753	Band 10	200	0.1745	0.7947	0.9237	0.0160	1.0015	0.0188
761	Band 11	200	0.0000	0.0000	NaN	0.2846	NaN	NaN
778	Band 12	200	0.0874	0.8945	0.8827	0.0192	1.0026	0.0230
865	Band 13	200	0.1859	0.7730	0.8577	0.0190	1.0023	0.0232
885	Band 14	200	0.2574	0.6801	0.8300	0.0197	1.0011	0.0246
900	Band 15	200	0.3658	0.5224	0.7974	0.0235	1.0001	0.0307

Table 2: The statistics of the retrieval of the BRDF coefficients over the Dome-C PICS.

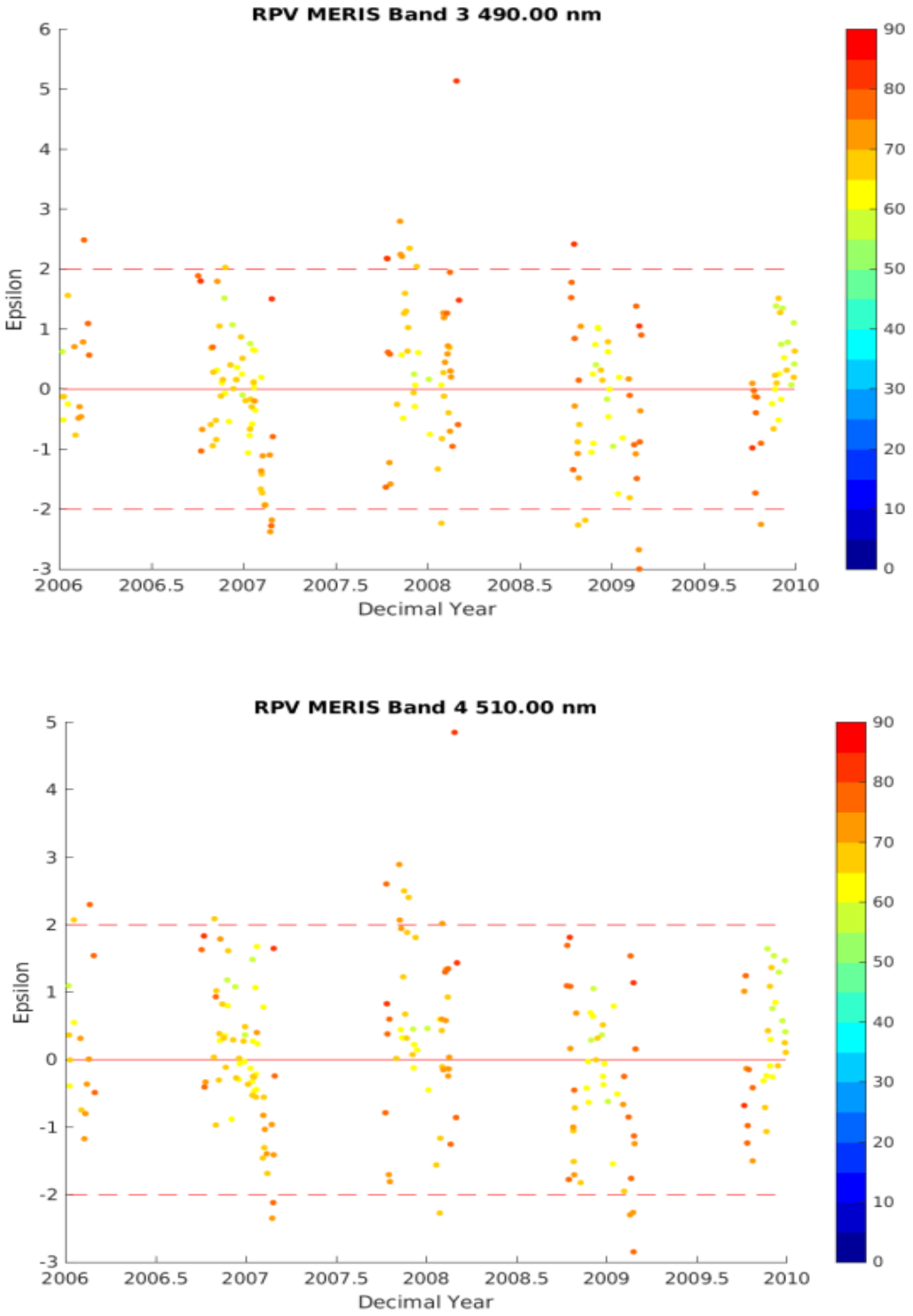

Figure 6. The Relative difference between MERIS TOA reflectance for band3 and band4 and their simulations using the inverted RPV parameters.

5. Generation of hyperspectral surface BRDF from MERIS surface BRDF model

Figure 7 and Figure 8 is used to fit the MERIS the ρ_0 parameter spectral variations. The spectral variations of the 3 other BRDF model parameters (k, Θ and the ratio $\omega = {\rho_c}/{\rho_0}$) are obtained by simple spline interpolation. The interpolation of the BRDF model parameters is done excluding spectral band for which the water vapour and O2 absorption is significant (band 11 and 15). The hyperspectral BRDF results are shown in Figure 5.

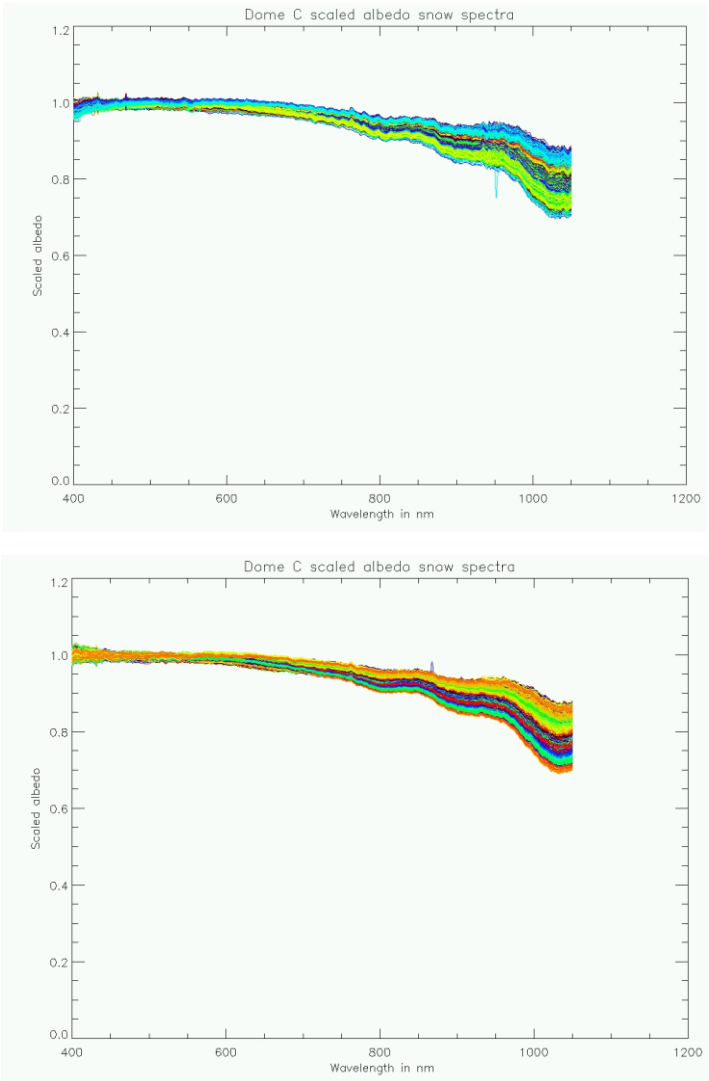

Figure 7: All albedo snow spectra measured over Dome-C from SAGE dataset (top) Head 1 x 3 seasons and (bottom) Head 2 x 3 seasons (Berthelot (2022); RD.3).

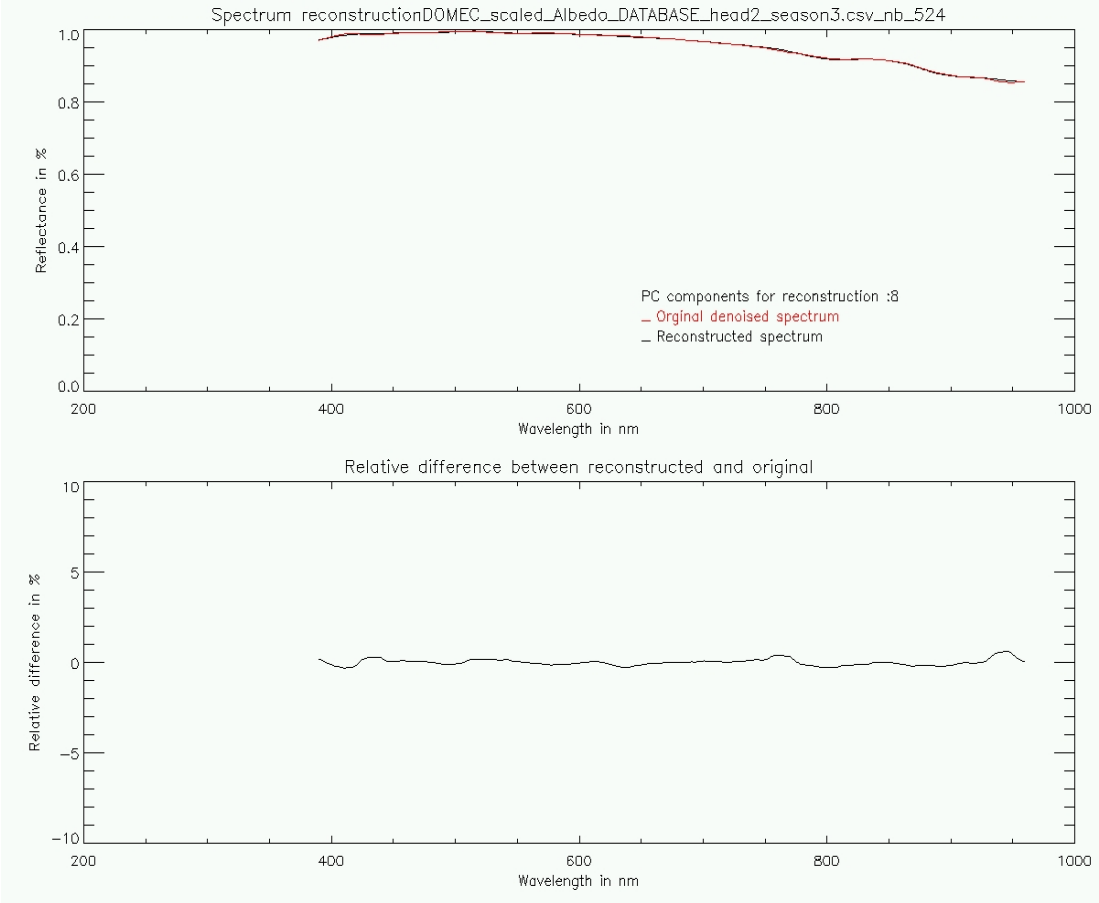

Figure 8: The spectral variations of the BRDF model parameter ρ_0 using 8 eigen vectors obtained from PCA or the full reflectance/albedo DB (denoised)

6. Simulation of TOA observations over the Dome-C for any sensor

The hyperspectral surface BRDF model and aerosol optical properties the Dome-C site described above can be used as input to simulate the hyperspectral TOA reflectance over the site which in turn, after convolution with the sensor spectral response can be used to simulate the in-band TOA reflectance of any sensor observing the sites, in any given geometry.

Only L1 data that are identified as cloud free in the ROI and quality checked in DIMITRI Database are compared to their simulations. Together with TOA reflectance, the illumination and observation geometry are extracted and used as input to the simulations.

The meteorological data (WV and O3) accompanying the sensor L1 data and extracted in DIMITRI are substituted by the corresponding ERA-Interim data.

7. Verification of the hyperspectral TOA simulations: Simulation of MERIS TOA observations over the Dome-C PICS

The full four years of MERIS TOA observations over the Dome-C PICS are used along with the hyperspectral BRDF model parameters (derived from the filtered 4 years of MERIS data only) to simulate the TOA over the site. This allows assessing the hyperspectral TOA reflectance model ability to reproduce the MERIS observations. Figure 9 shows the time series of the ratio $\frac{\rho_{obs}^{TOA}(\lambda)}{\rho_{sim}^{TOA}(\lambda)}$ over the Dome-C CEOS PICS site over 2006-2009 of MERIS 3rd reprocessing data. The mean values of the ratio and associated standard deviations obtained over all 6 PICS sites are provided in Table 3 in a spectral synthesis.

These results are further discussed in the following sections.

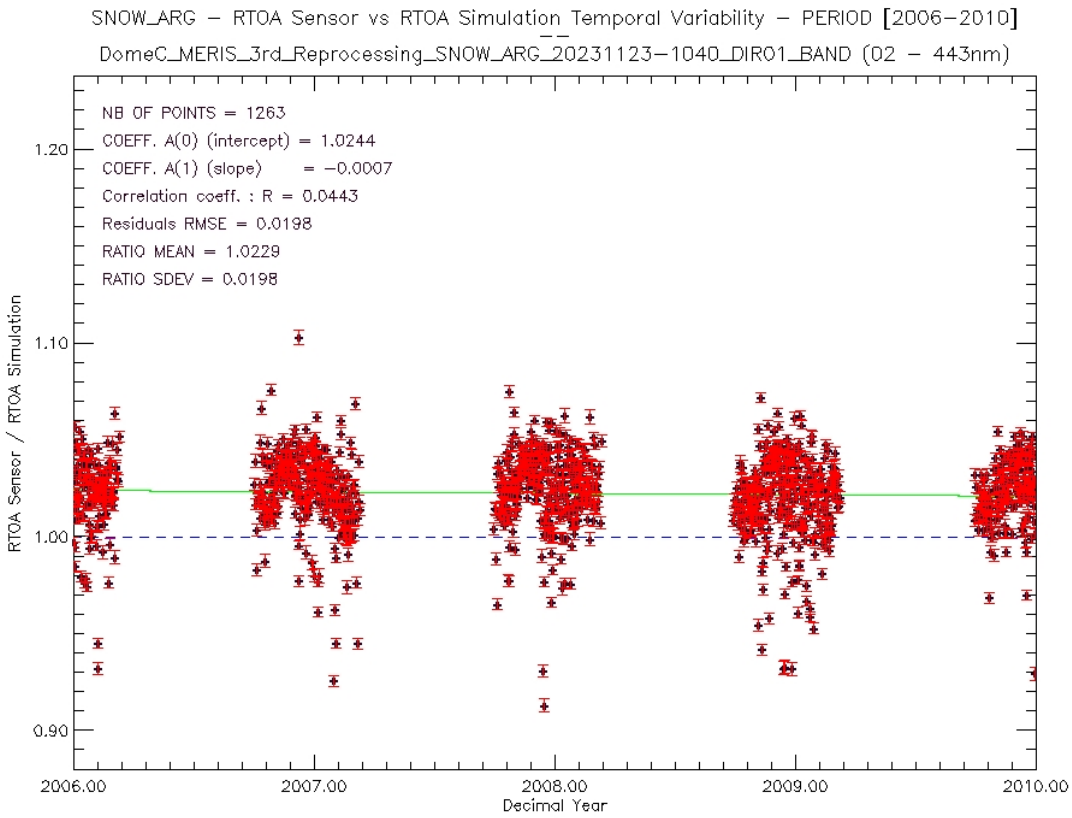

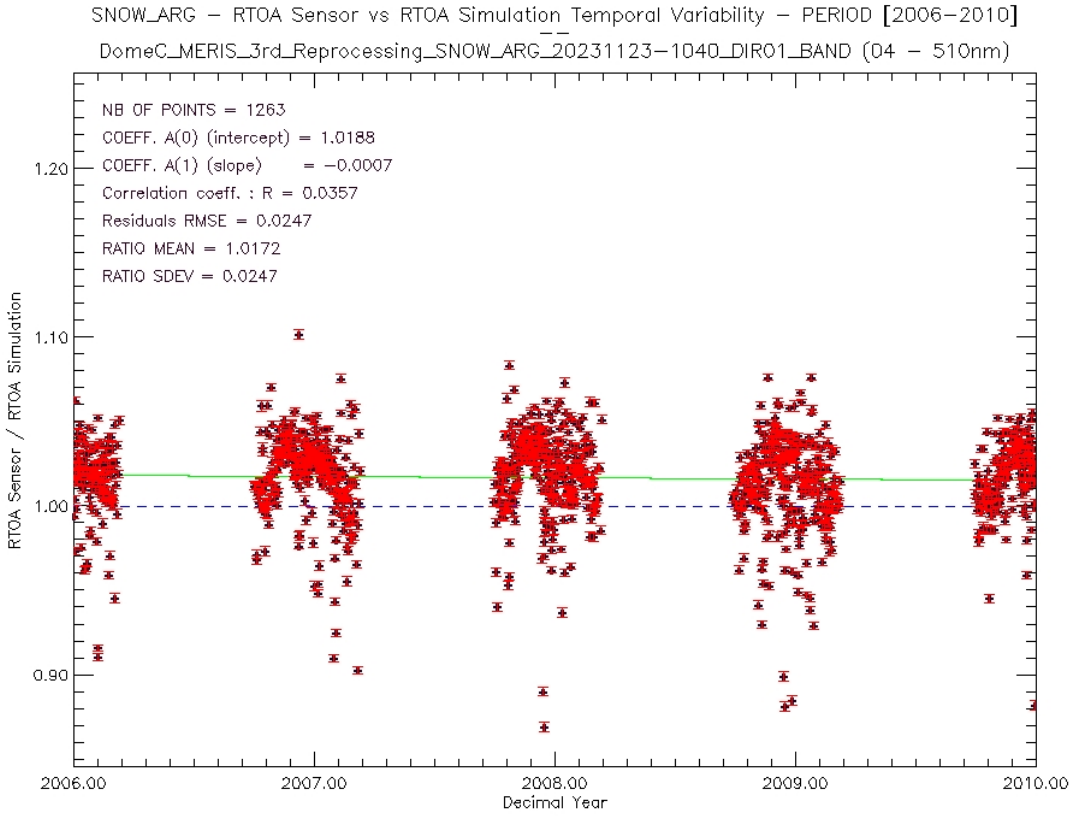

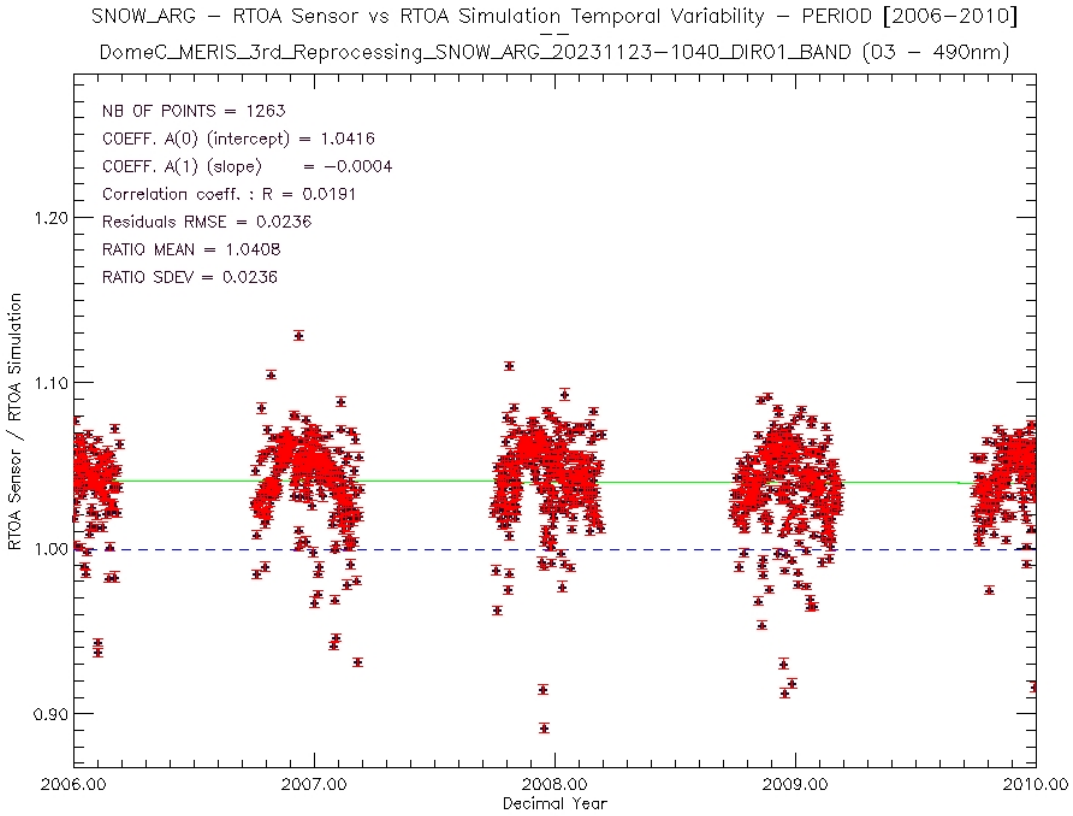

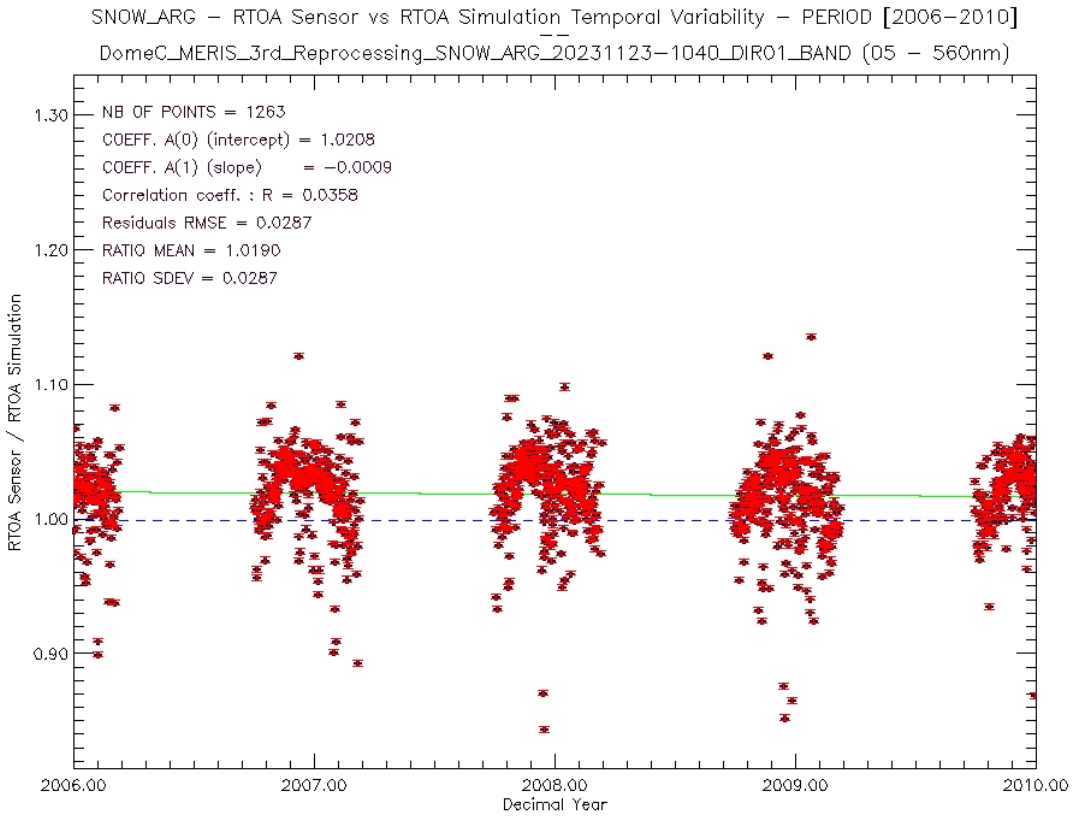

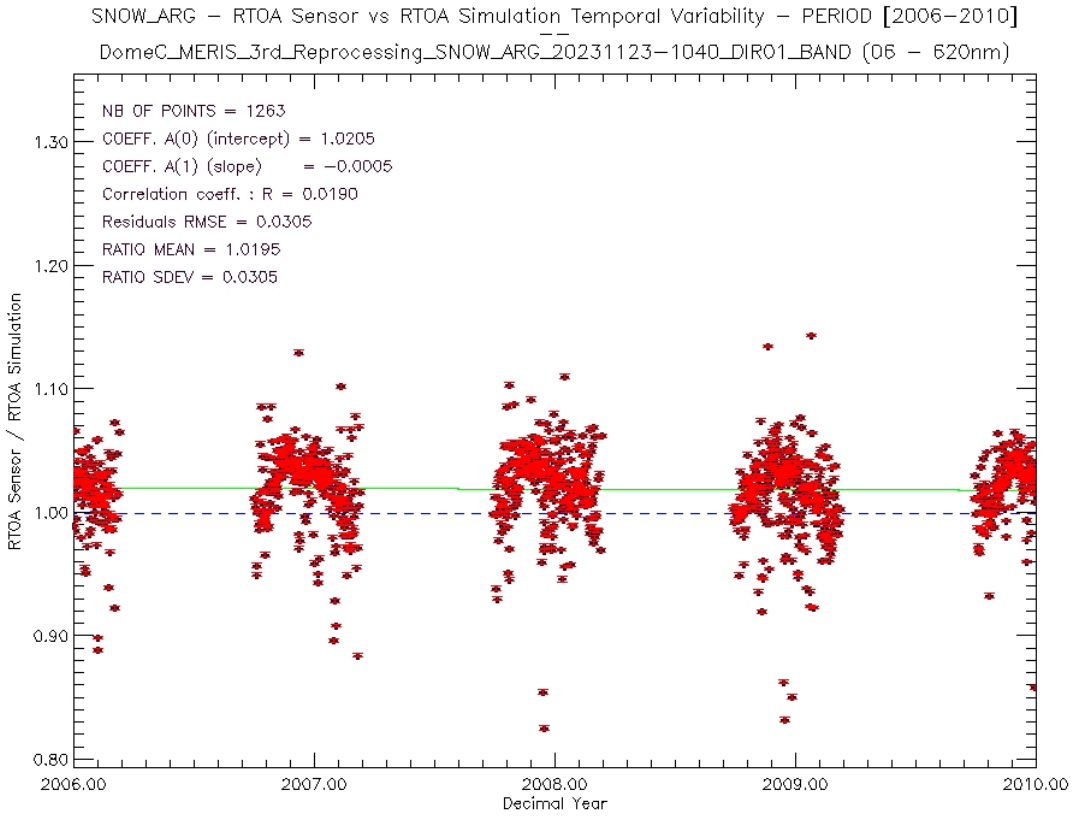

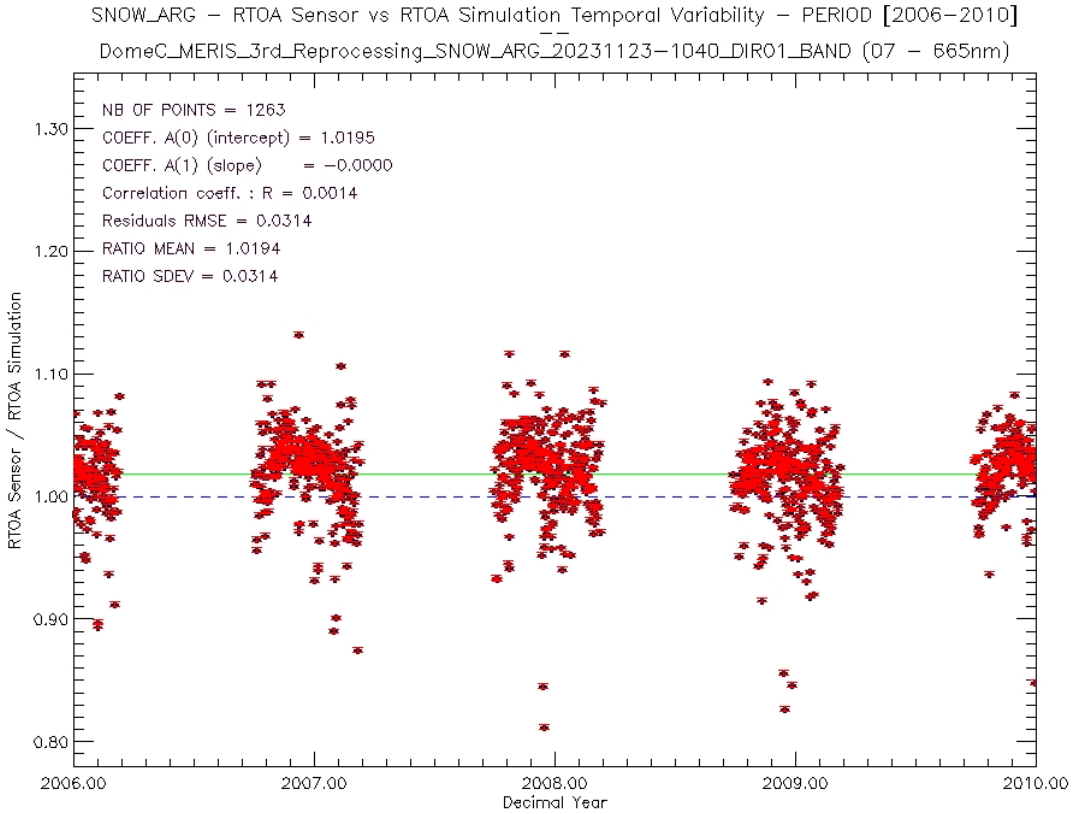

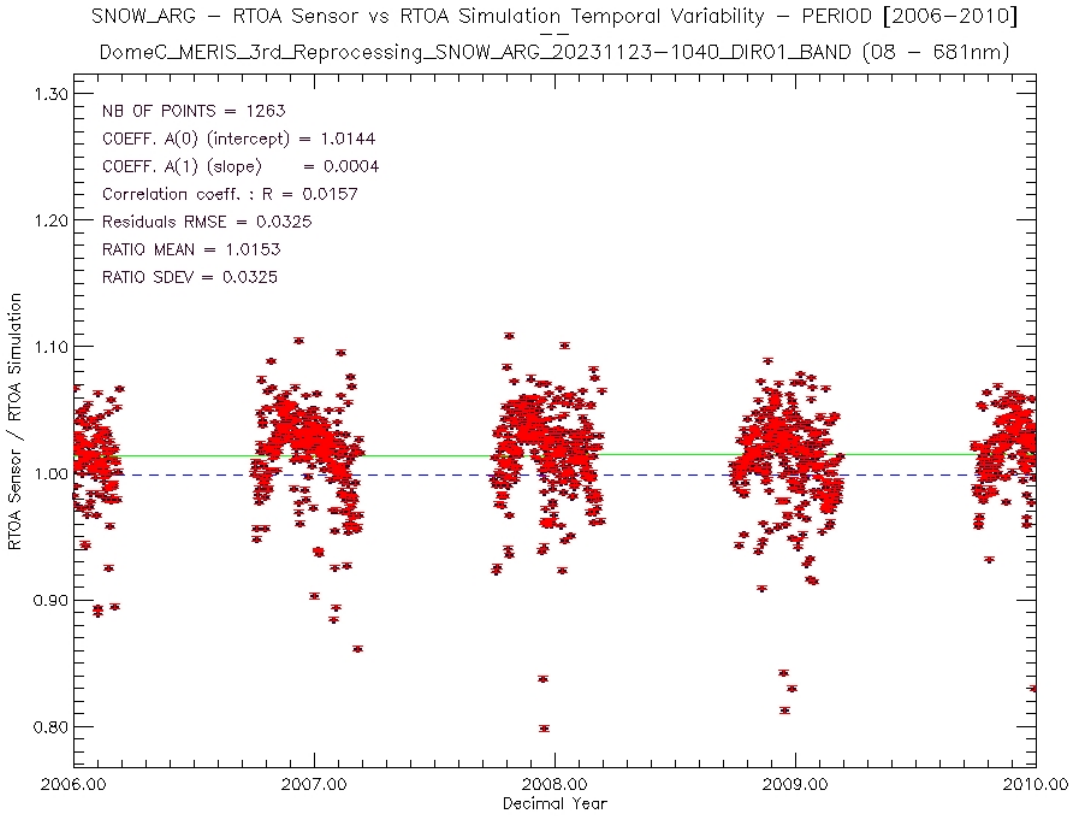

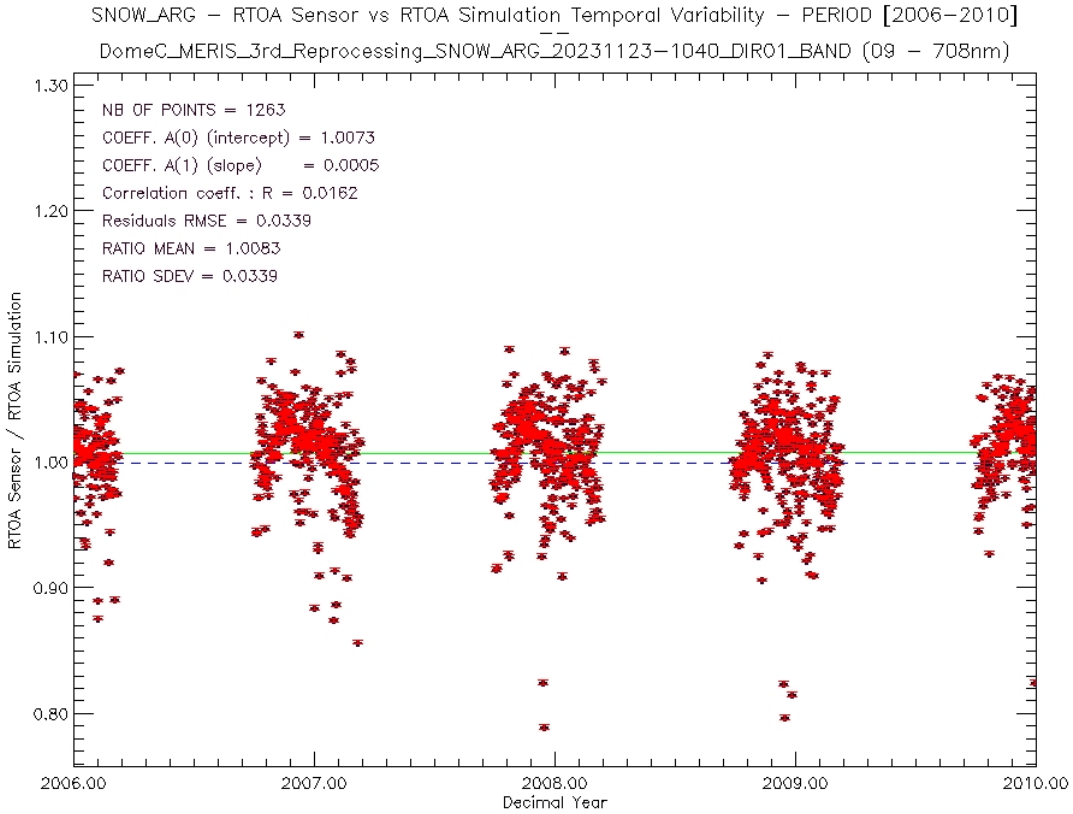

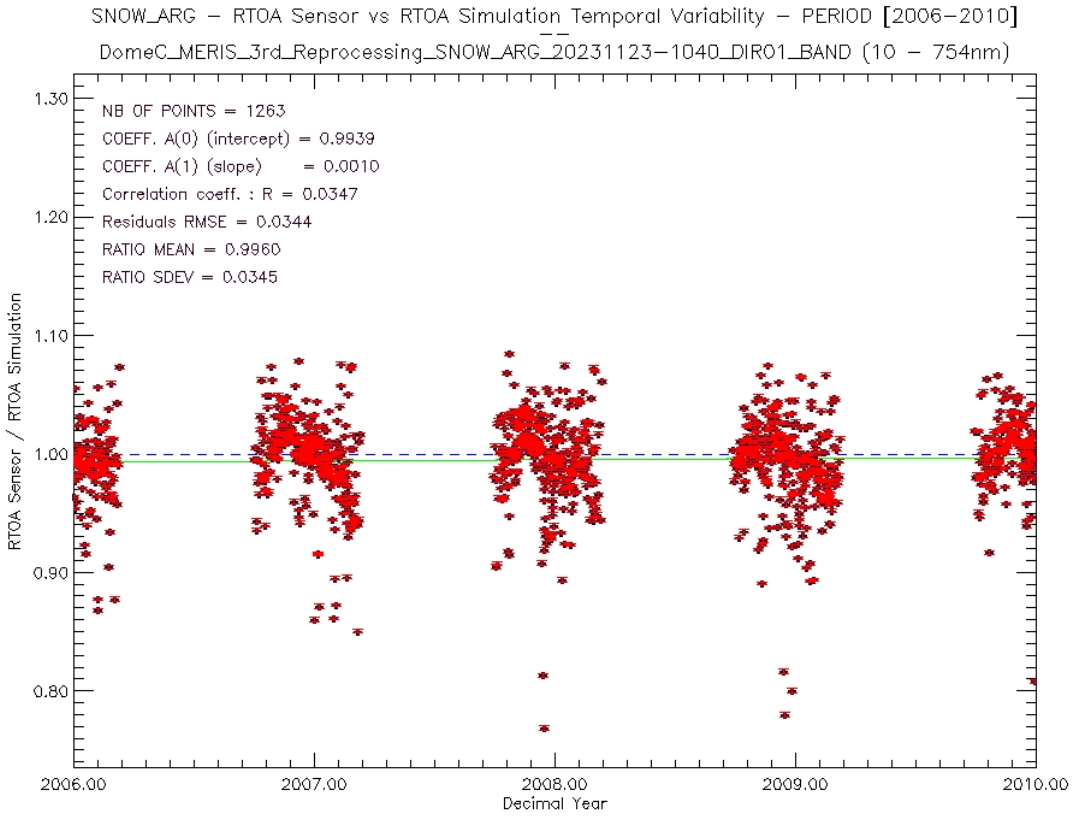

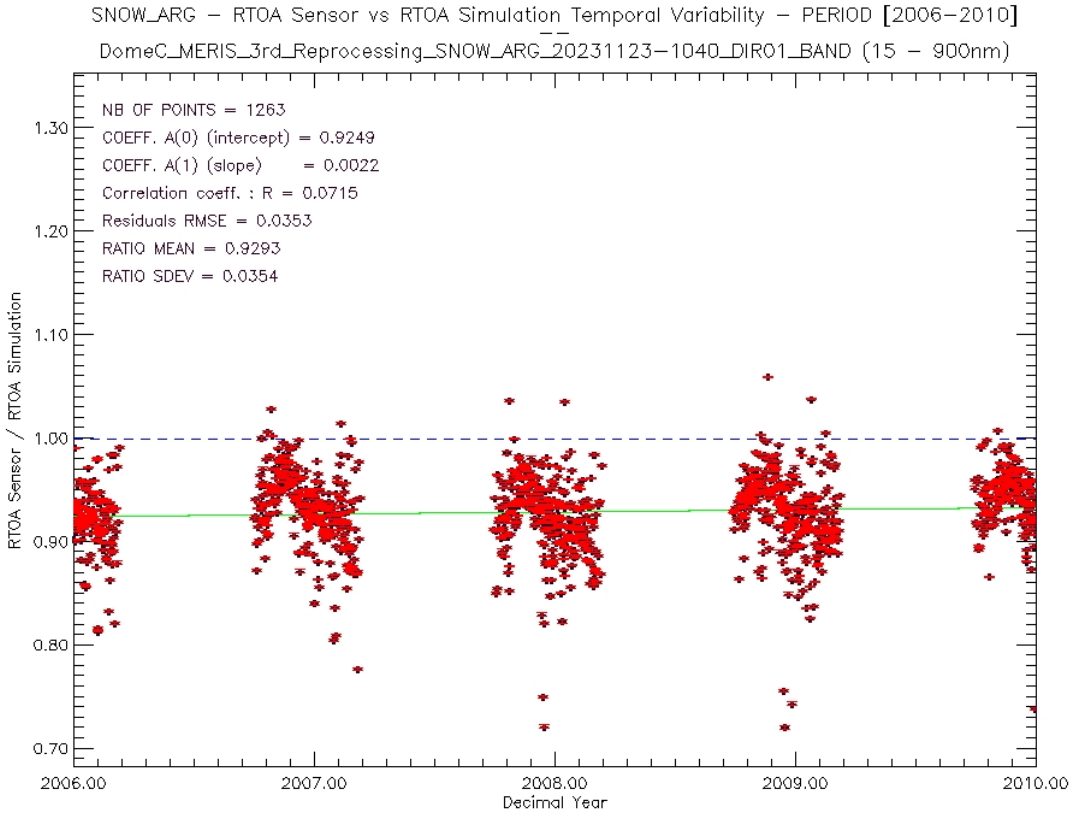

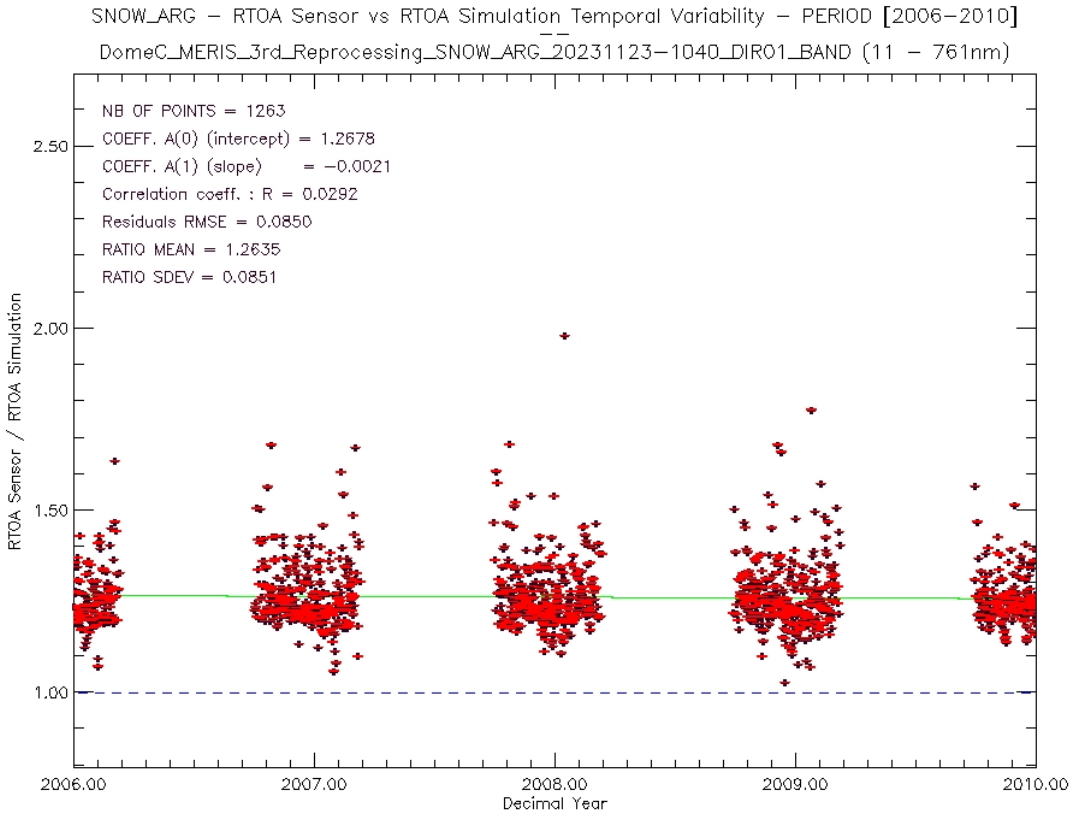

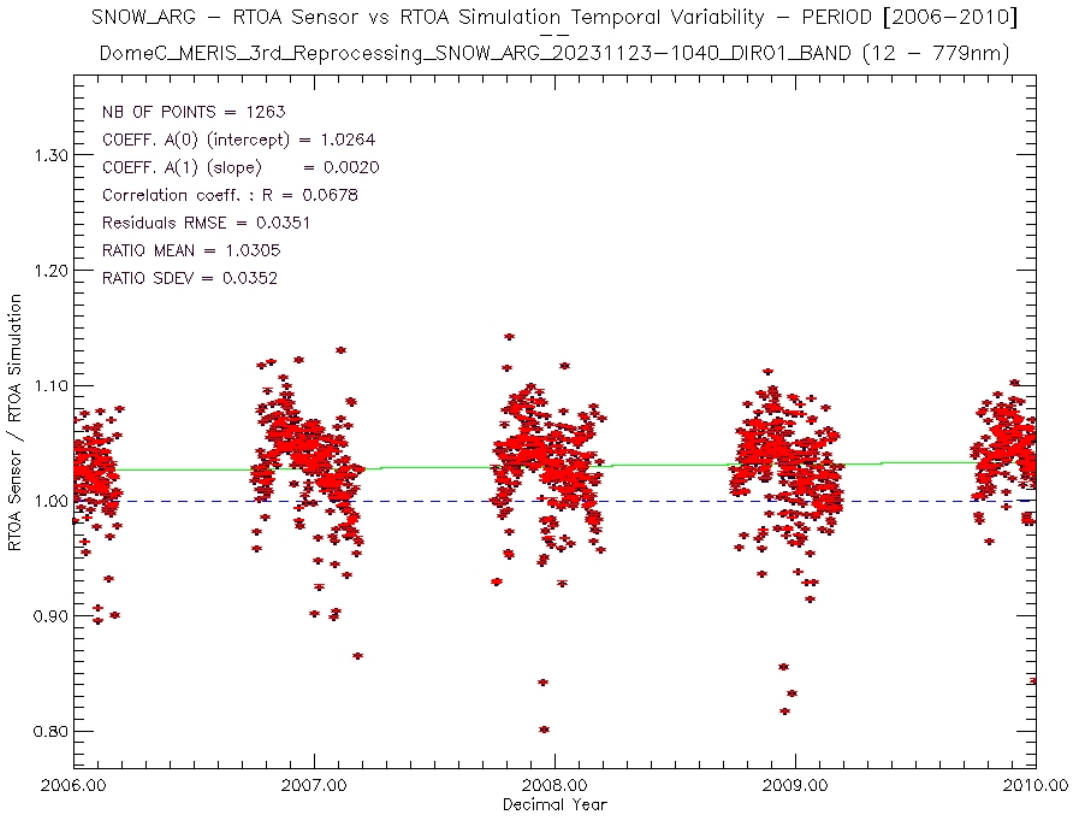

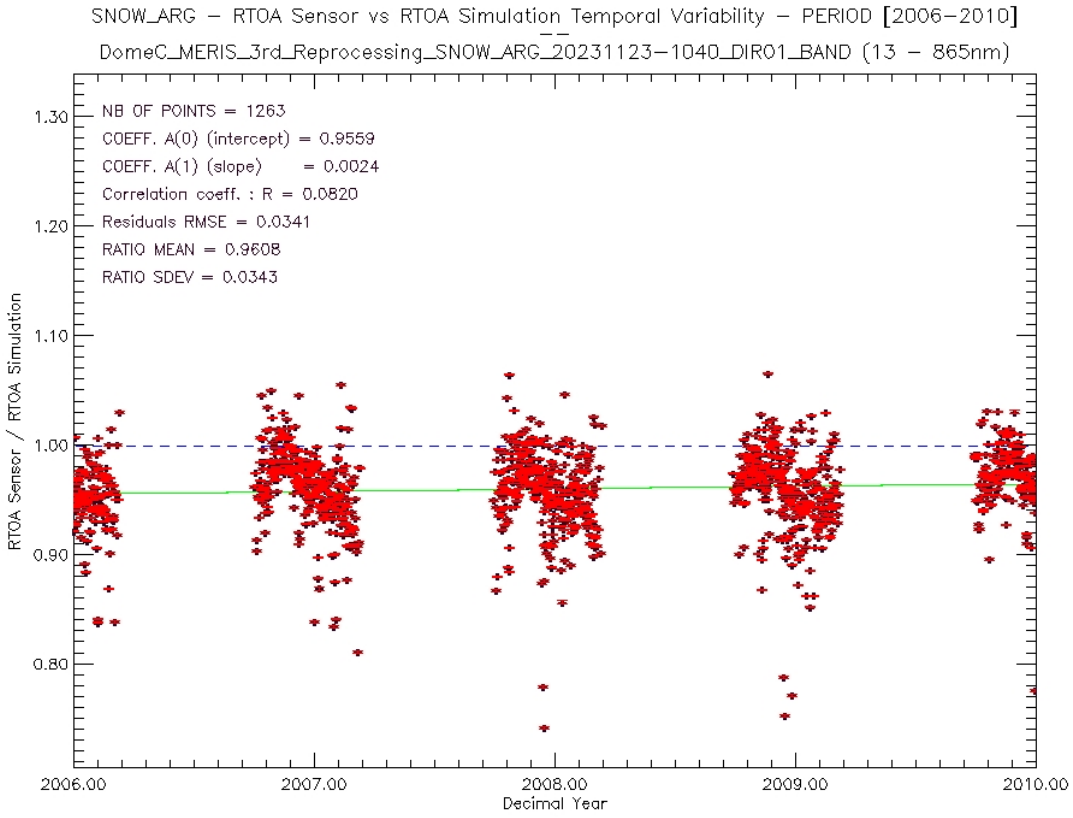

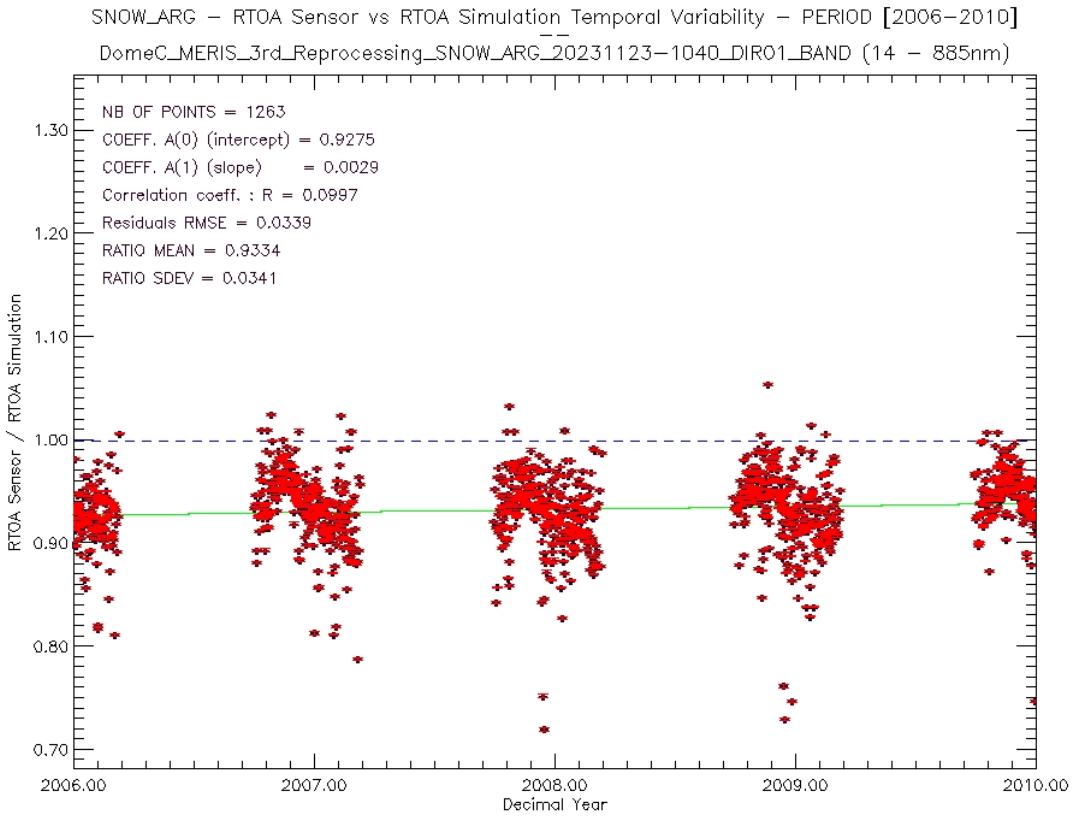

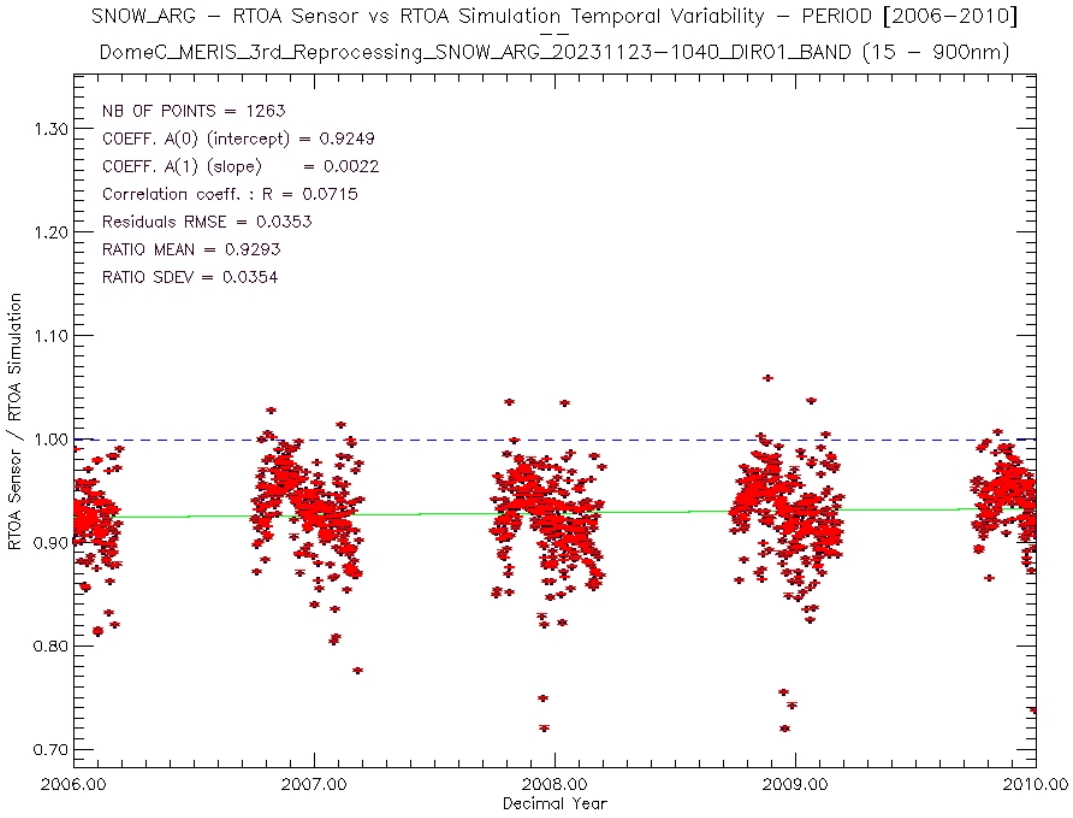

Figure 9: The temporal variations of the ratio $\frac{\rho_{obs}^{TOA}(\lambda)}{\rho_{sim}^{TOA}(\lambda)}$ for MERIS 3rd reprocessing band01- band15 over the Dome-C PICS site identified by CEOS.

ARG MERIS								
WL (nm)	**Band**	**NB Points**	**A(0) Intercept**	**A1 Slope**	**R**	**RMSE**	**Mean Ratio**	**STD**
412	Band 1	1263	1.0115	-0.0009	0.0633	0.0173	1.0096	0.0173
443	Band 2	1263	1.0244	-0.0007	0.0433	0.0198	1.0229	0.0198
490	Band 3	1263	1.0416	-0.0004	0.0191	0.0236	1.0408	0.0236
510	Band 4	1263	1.0188	-0.0007	0.0357	0.0247	1.0172	0.0247
560	Band 5	1263	1.0208	-0.0009	0.0358	0.0287	1.0190	0.0287
620	Band 6	1263	1.0205	-0.0005	0.0190	0.0305	1.0195	0.0305
665	Band 7	1263	1.0195	0.0000	0.0014	0.0314	1.0194	0.0314
681	Band 8	1263	1.0144	0.0004	0.0157	0.0325	1.0153	0.0325
708	Band 9	1263	1.0073	0.0005	0.0162	0.0339	1.0083	0.0339
753	Band 10	1263	0.9939	0.0010	0.0347	0.0344	0.9960	0.0345
761	Band 11	1263	1.2678	-0.0021	0.0292	0.0850	1.2635	0.0851
778	Band 12	1263	1.0246	0.0020	0.0687	0.0351	1.0305	0.0352
865	Band 13	1263	0.9559	0.0024	0.0820	0.0341	0.9608	0.0343
885	Band 14	1263	0.9275	0.0029	0.0997	0.0339	0.9334	0.0341
900	Band 15	1263	0.9249	0.0022	0.0715	0.0353	0.9293	0.0354

Table 3: The mean values of the ratio $\frac{\rho_{obs}^{TOA}(\lambda)}{\rho_{sim}^{TOA}(\lambda)}$ for MERIS 3rd reprocessing 2006-2009 averaged over the Dome-C PICS site identified by CEOS and its associated statistics.

8. Known limitations of the TOA simulations

8.1. Retrieval of BRDF model parameters in the MERIS spectral bands with significant water vapour and O2 absorption

The retrieval of BRDF model parameters over the Dome-C PICS in the MERIS spectral bands with significant absorption from O2 results into larger RMSE between the simulated and measured MERIS observations 761 nm than in neighbouring spectral bands not sensitive to absorption from this gas (see the last three columns in Table 3). In addition to this band, the NIR bands where wavelengths are higher than 880 nm show biases higher than 5%, although its RMSE are twice lower than the RMSE for band 11. There are two explanations for this larger residual RMSEs. First, the absorption cross sections used for the modelling of these gases might be inaccurate. Second, there is an additional variability in the TOA reflectance at 761 nm and 900 nm (both bands are excluded from the BRDF fit). Water vapour absorption is influenced by the natural spatio-temporal variability water vapour concentration. This might not be sufficiently well captured by the ERA-Interim water vapour fields. O2 absorption is mostly influenced by surface pressure variations that are not accounted for in the TOA simulations. Moreover, other physical factors might influence the absorption in both bands such as the atmospheric temperature and aerosol optical properties and vertical distribution.

These bands were thus excluded from the bands used to retrieve the hyperspectral BRDF model parameters and the parameters values obtained at 761 and 900 nm from MERIS observations (black stars in the Figure 5) are often seen to depart from the hyperspectral model (red line in Figure 5)

8.2. Spectral interpolation of the surface BRDF model between the MERIS spectral bands

The full dataset of MERIS TOA observations over 2006-2009 over the Dome-C have been used along with the hyperspectral BRDF model parameters (derived from 4 years of MERIS filtered data only) to measure the performance of the model, i.e., it's ability to reproduce the MERIS observations over the full dataset (Figure 9 and Table 3). One would expect that the MERIS simulated TOA-reflectance obtained using the hyperspectral BRDF models retrieved over each PICS as input to the simulation should allow reproducing the MERIS TOA observations to within the RMSE and the accuracy indicated in Table 2.

Figure 9 shows that this is not always the case in the absorption bands at 761 and 900 nm (for the reasons detailed in the previous section).

One can also observe that at 490 nm, 865 and 885 nm (Figure 9), the simulation of MERIS TOA observations are not consistent with those obtained at other bands, this might be explained by the lower TOA Reflectance at these bands (Figure 8).

9. Uncertainties of the TOA simulations

9.1. Spectral bands with marginal water vapour and O2 absorption

We can distinguish the random and systematic uncertainty associated to the simulations of TOA reflectances.

9.1.1. Random uncertainties estimation

The random uncertainty associated to the TOA simulation of sensors with spectral bands without significant absorption from water vapour and O2 should be of the same order of the RMSE obtained in the spectral bands of MERIS, i.e, in the range of 1% to 2% (Table 2). This is confirmed by the standard deviations associated to $\frac{\rho_{obs}^{TOA}(\lambda)}{\rho_{sim}^{TOA}(\lambda)}$ time series obtained on the full dataset 2006-2009 MERIS 3REP over Dome-C site in Table 3

The random uncertainty assigned to each acquisition simulation for any site and any wavelength not affected by water vapour or O2 absorption is thus conservatively estimated to 2 % (k=1) or 4% (k=2).

9.1.2. Systematic uncertainties estimation

The systematic uncertainties associated to the TOA simulations over a given site have two origins:

1. The residual bias after the surface BRDF model parameters in MERIS bands were retrieved (see the mean ratios in Table 2). This is below 1% and varies from band to band.
2. The mismatch between the hyperspectral BRDF parameters and the same parameters derived from the inversion of the MERIS reference data at the MERIS spectral band central wavelengths. This is due to the fact that the derivation of the hyperspectral ρ_0 variations is based on a least square fit between the 13 MERIS spectral ρ_0 values and 8 linearly combined *eigen* spectral from the hyperspectral database of surface reflectance.

In both cases, the systematic uncertainty contributors should be site dependant and using several sites should reduce the systematic uncertainty from a single site. When using only individual site, the systematic uncertainty can reach ~ 4% as discussed above for all bands not affected by water vapour and O2 absorption.

9.2. Spectral bands with significant water vapour and O2 absorption: 761 nm and 900 nm

9.2.1. Random uncertainties estimation

The random uncertainty associated to the TOA simulation of sensors with spectral bands with significant absorption from water vapour and O2 should be of the same order of the RMSE obtained in the spectral bands of MERIS, i.e, in the range of 4%-8% (Table 3).

The random uncertainty assigned to each acquisition simulation for any site is thus conservatively set to 8 % (k=1) or 16% (k=2).

9.2.2. Systematic uncertainties estimation

The systematic uncertainty associated to the TOA simulation of sensors with spectral bands with significant absorption from water vapour and O2 is more difficult to assess. It was previous discussed that it might have different origins (inaccuracy of the absorption cross-sections, non-modelled atmospheric temperature/pressure variability and vertical distribution). It was rather set to

conservative values roughly commensurate with the level of absorption in these spectral bands: 50 % for bands 761 and 900 nm.

10. Conclusion

Hyperspectral BRDF model parameters were derived for the Dome-C CEOS PICS from 4 years of MERIS 3rd reprocessing data.

These hyperspectral BRDF model parameters can be used in DIMITRI to simulate TOA reflectance for any sensor.

The uncertainty budget was broken down into system and random uncertainties for spectral regions with or without water vapour and O2 absorption.

References

- Bouvet M., Radiometric comparison of multispectral imagers over a pseudo-invariant calibration site using a reference radiometric model, *Remote Sensing of Environment 140 (2014) 141–154.*

- Breon, F.-M. and Maignan, F.: A BRDF–BPDF database for the analysis of Earth target reflectances, Earth Syst. Sci. Data, 9, 31–45, https://doi.org/10.5194/essd-9-31-2017, 2017.

- Cosnefroy, H., Leroy, M. and Briottet, X. (1996). Selection of Sahara and Arabia desert sites for the calibration of optical satellite sensors. Remote Sensing of the Environment, 58, 101-114

- Hess, M., Koepke, P., & Schult, I. (1998). Optical properties of aerosols and clouds: The software package OPAC. Bulletin of the American Meteorological Society, 79, 831–844.

- Rahman, H., Pinty, B., & Verstraete, M. M. (1993). Coupled surface-atmosphere reflectance (CSAR) model, 2, Semi empirical surface model usable with NOAA advanced very high-resolution radiometer data, Journal of Geophysical Research, 98(D11), 20,781–20,801, 1993a.

- Rahman, H., Verstraete, M., and Pinty, B. (1993). Coupled surface-atmosphere reflectance (CSAR) model. 1. Model description and inversion on synthetic data, Journal of Geophysical Research, 98, 20 779–20 789, 1993b.